Double Photonic Quasi-Crystal Structure Effect on GaN-Based Vertical-Injection Light-Emitting Diodes

2010 Jpn. J. Appl. Phys. 49 022101

(http://iopscience.iop.org/1347-4065/49/2R/022101)

Japanese Journal of Applied Physics 49 (2010) 022101 **REGULAR PAPER**

Double Photonic Quasi-Crystal Structure Effect on GaN-Based Vertical-Injection Light-Emitting Diodes

Hung-Wen Huang[1,2*], Chung-Hsiang Lin[2], Zhi-Kai Huang[1], Kang-Yuan Lee[2], Chang-Chin Yu[2], and Hao-Chung Kuo[1]

[1] *Institute of Electro-Optical Engineering, National Chiao-Tung University, Hsinchu 30050, Taiwan, R.O.C.*
[2] *Luxtaltek Corporation, Chunan, Miaoli 350, Taiwan, R.O.C.*

Received June 13, 2009; accepted October 30, 2009; published online February 22, 2010

GaN-based thin-film vertical-injection light-emitting diodes (VLEDs) with a double 12-fold photonic quasi-crystal (PQC) structure formed using nanoimprint lithography (NIL) and inductively coupled plasma reactive-ion etching (ICP-RIE) are fabricated and presented. At a driving current of 20 mA and with a chip size of 350 x 350 μm^2, our thin-film LED with a double-12-fold-PQC structure gave a light output power of 40.5 mW, which is an increase of 77% when compared with the output power of a VLED without a PQC structure at a peak wavelength of 460 nm. In addition, the corresponding light radiation patterns show a narrow beam shape due to the strong guided light extraction on the n-GaN surface and the reflected light effect of the PQC structure formed in the vertical direction on the p-GaN surface.

DOI: 10.1143/JJAP.49.022101

1. Introduction

GaN-based materials have attracted considerable interest in many optoelectronic device applications, such as light-emitting diodes (LEDs) and laser diodes (LDs). Recently, high-brightness GaN-based LEDs have been applied in outdoor displays, traffic signals, LED-backlit liquid crystal displays, and direct-view large-area signage.[1–3] To extend the applications of GaN-based LEDs in projectors, automobile headlights, and even general lighting, further improvements in optical power and light extraction efficiency are required. The thin-film LED structure has been developed very recently and is a promising candidate for achieving the above goal. A well-known thin-film GaN LED structure is fabricated by removing the sapphire layer using an excimer laser[4–6] and roughening the revealed n-doped GaN layer.[7] Recently, we have reported an increase in the extraction efficiency of GaN-based LEDs prepared by surface roughening.[8,9] To improve the light scattering effect or extraction efficiency of a roughened surface, various methods of fabricating nanostructures on the GaN surface have been reported. Examples of structures fabricated are GaN nanorods formed using inductively coupled plasma reactive-ion etching (ICP-RIE) with a nanomask,[10] dislocation-free InGaN/GaN multiple-quantum-well (MQW) nanorod arrays grown by metalorganic-hydride vapor phase epitaxy (MO-HVPE),[11] nanoporous GaN:Mg structures fabricated by photochemical etching (PEC),[12] InGaN/GaN nanoposts prepared by e-beam lithography,[13] and GaN-based LEDs with a nanoetched sapphire substrate prepared by metalorganic chemical vapor deposition (MOCVD).[14] To maximize the light scattering performance of nanostructures, we employ a nanoimprint lithography (NIL) technique of fabricating double-photonic-quasi-crystal structures on GaN vertical-injection LED epitaxial film. Furthermore, to demonstrate ultrahigh-brightness GaN-based LEDs, the electrical and optical characteristics of a thin-film vertical-injection LED incorporated with 12-fold PQC structures by NIL are presented.

2. Experimental Procedure

The experimental GaN-based LED samples are grown by MOCVD with a rotating-disk reactor (Veeco) on a *c*-axis sapphire (0001) substrate at a growth pressure of 200 mbar. Our prepared GaN LED wafer consists of a 50-nm-thick GaN nucleation layer grown at 550 °C, a 2-μm-thick undoped GaN buffer layer grown at 1050 °C, a 3-μm-thick Si-doped n-GaN layer grown at 1050 °C, an unintentionally doped InGaN/GaN MQW active region grown at 770 °C, a 50-nm-thick Mg-doped p-AlGaN electron blocking layer grown at 1050 °C, and a 0.2-μm-thick Mg-doped p-GaN contact layer grown at 1050 °C. The MQW active region consists of five periods of 3-/7-nm-thick $In_{0.21}Ga_{0.79}N$/GaN quantum well layers and barrier layers. Figures 1(a)–1(d) show four schematic diagrams for comparison: (a), GaN VLED without PQC pattern structures; (b), GaN VLED with PQC pattern structures on p-GaN surface; (c), GaN VLED with PQC structures on n-GaN surface; and (d), GaN VLED with double-PQC structures on the p- and n-GaN surfaces. The following is a detailed process flow of NIL on a p-GaN surface. First, we spin-coated a 200-nm-thick polymer layer on the p-GaN surface. Second, we placed a patterned mold onto the dried polymer film. By applying a high pressure, we heated the LED samples to a temperature above the glass transition temperature of the polymer. Third, the LED samples and mold were then cooled to room temperature to release the mold. Finally, we used ICP-RIE with Cl_2/BCl_3/Ar plasma to transfer the pattern onto the p-GaN layer and remove the polymer layer with O_2 plasma etching gas in an RIE system.

The double-PQC structure process of fabricating a GaN VLED is described as follows: First, a transparent contact of a Ni/Au (3/3 nm) layer, a silver (Ag) mirror, and a bonding metal layer of Cr/Pt/Au (50/30/1400 nm) are respectively deposited onto the p-GaN layer of our prepared LED wafer. The deposited LED wafer is then bonded to a Cr/Pt//Au(50/30/1400 nm)-coated p-type conducting Si substrate using a commercial SUSS SB6e wafer bonder at a bonding temperature of 350 °C and a bonding pressure of 17 kg/cm^2 for 120 min. Second, the sapphire substrate of the bonded wafer is removed by a laser lift-off (LLO) process. In our experiment, we use a KrF excimer laser at a wavelength of 248 nm with a pulse width of 25 ns. The incident laser with a beam size of 1.2×1.2 mm^2 is incident from the polished back surface of the sapphire substrate to the sapphire/GaN interface to decompose GaN into Ga and N_2. In this LLO process, the beam size of the KrF laser is larger than our desired size (350×350 μm^2) of LEDs;

*E-mail address: stevinhuang737672@msn.com

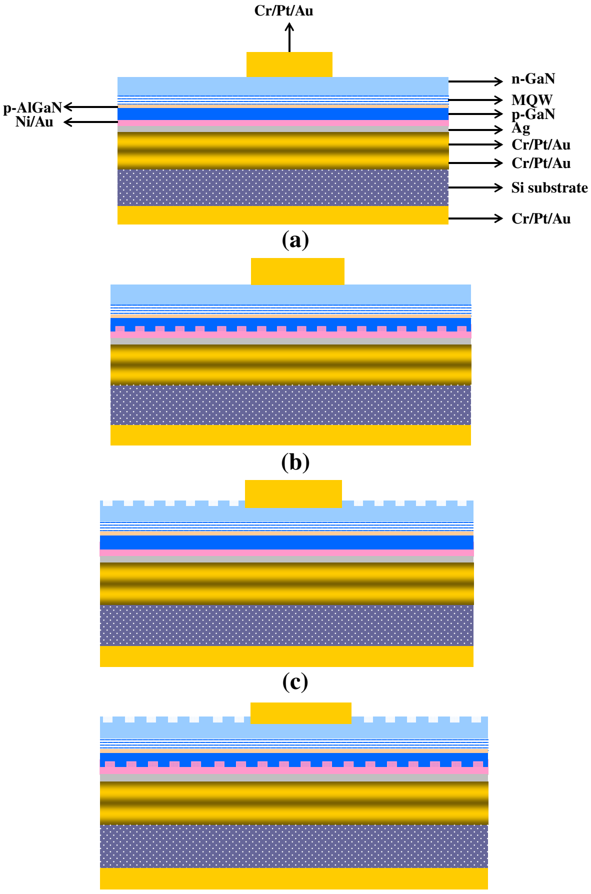

Fig. 1. (Color online) Schematic diagram (cross-sectional views) of a GaN VLED with four configurations: (a) conventional VLED, (b) VLED with PQC pattern structures on p-GaN surface, (c) VLED with PQC structures on n-GaN surface, (d) VLED with double-PQC structures on the p-GaN and n-GaN surfaces.

therefore, the laser irradiation at the interface of sapphire and GaN is rather uniform. Third, the sapphire-removed bonded wafer is dipped in HCl solution to remove residual Ga on the u-GaN. In order to thin out the revealed n-GaN, the whole sapphire-removed wafer is etched under the etching following conditions: a gas mixture of $BCl_3/Cl_2/Ar = 10/15/5$ sccm with ICP source power/bias power set at 100/150 W, and a chamber pressure of 2.25 mTorr with an approximate etching depth of 2 μm by ICP-RIE. Fourth, a 100-nm-thick SiO_2 layer is deposited onto the n-GaN surface by plasma enhanced chemical vapor deposition (PECVD) for PQC patterning. We then spin-coated a polymer layer on top of the SiO_2 layer and placed a patterned mold with a 12-fold PQC design onto the dried polymer film. By applying a high pressure, we heated the LED samples to a temperature above the glass transition temperature of the polymer. The LED samples and mold are then cooled to room temperature to release the mold. We then used RIE with CF_4 plasma to remove the residual polymer layer and transfer the pattern onto the SiO_2 layer. After the n-GaN etching, a buffer oxidation etchant (BOE) is used to remove the residual SiO_2 layer. Fifth, the associated mesas are etched further into the Ni metal interface using a SiO_2 etching mask by PECVD for single-chip isolation and then using a BOE to remove the residual SiO_2 layer. Sixth, a 300-nm-thick SiO_2 layer is deposited onto the wafer surface and photolithography is then used to define the passivation pattern after the wet etching of SiO_2 by BOE. Finally, a patterned Cr/Pt/Au electrode is deposited onto the n-GaN layer as the n-type contact layer and Cr/Pt/Au metal is deposited onto the Si substrate surface. To examine the etching depth and dimension size of the PQC structure, field-emission scanning electron microscopy (FESEM; Hitachi S-5000) is performed.

3. Results and Discussion

Figures 2(a)–2(d) show cross-sectional and top-view SEM images of our designed 12-fold PQC based on a square-triangular lattice [inset shows the model on the right-hand-side of Fig. 2(b)]. Figure 2(a) shows the PQC etching depth and sidewall angle of the p-GaN layer to be approximately 80 nm and 75°, respectively. In Fig. 2(b), the lattice constant and hole diameters are 450 and 275 nm, respectively. The PQCs are unique in that at first glance they appear random; however; closer inspection reveals them to possess long-range order but short-range disorder.[15,16] We choose the 12-fold PQC pattern owing to its capability to better enhance surface emission. The pattern is obtained from photonic crystals (PhCs) with a dodecagonal symmetric quasi-crystal lattice, and not from regular PhCs with a triangular lattice or from an 8-fold PQC.[15] The recursive tiling of offspring dodecagons packed with random ensembles of squares and triangles in dilated parent cells forms the lattice shown on the right-hand-side of Fig. 2(b). Figure 2(c) shows the PQC etching depth and sidewall angle of the n-GaN layer to be approximately 260 nm and 50°, respectively. In Fig. 2(d), the lattice constants and hole diameters of the n-GaN surface are 450 and 245 nm, respectively.

The light outputs of our samples are detected by calibrating an integrating sphere with a Si photodiode on an LED wafer device with a peak wavelength of 460 nm. Figure 3(a) shows the typical current–voltage (I–V) characteristics. The measured forward voltages at an injection current of 20 mA at room temperature for the conventional VLED, the VLED with a PQC pattern on p-GaN, the VLED with a PQC pattern on n-GaN, and the VLED with a double-PQC pattern are 3.23, 3.27, 3.27, and 3.29 V, respectively. Furthermore, in our experiments, the dynamic resistances ($R = dV/dI$) of the VLED with a PQC pattern on p-GaN, the VLED with a PQC pattern on n-GaN, and the VLED with a double-PQC pattern are 17, 18, and 18 Ω, respectively; which are 6–12% higher than that of the conventional VLED (16 Ω). Therefore, in terms of dynamic resistance, incorporating a PQC pattern structure using NIL and an ICP process on these types of devices has only a small effect. The inset of Fig. 3(a) shows the typical room-temperature electroluminescence (EL) spectra of GaN-based LEDs with and without a PQC pattern at a driving current of 20 mA. We can see that the GaN-based MQW emission peaks of such devices are located at 460 nm. Furthermore, the EL intensities of the LED with a PQC pattern are larger than that of the conventional LED.

The intensity–current (L–I) characteristics of our four different types of VLED packaged on transistor outline (TO) cans are shown in Fig. 3(b). As expected, the light output powers of the VLED with a PQC pattern on p-GaN, the VLED with a PQC pattern on n-GaN, and the VLED with a

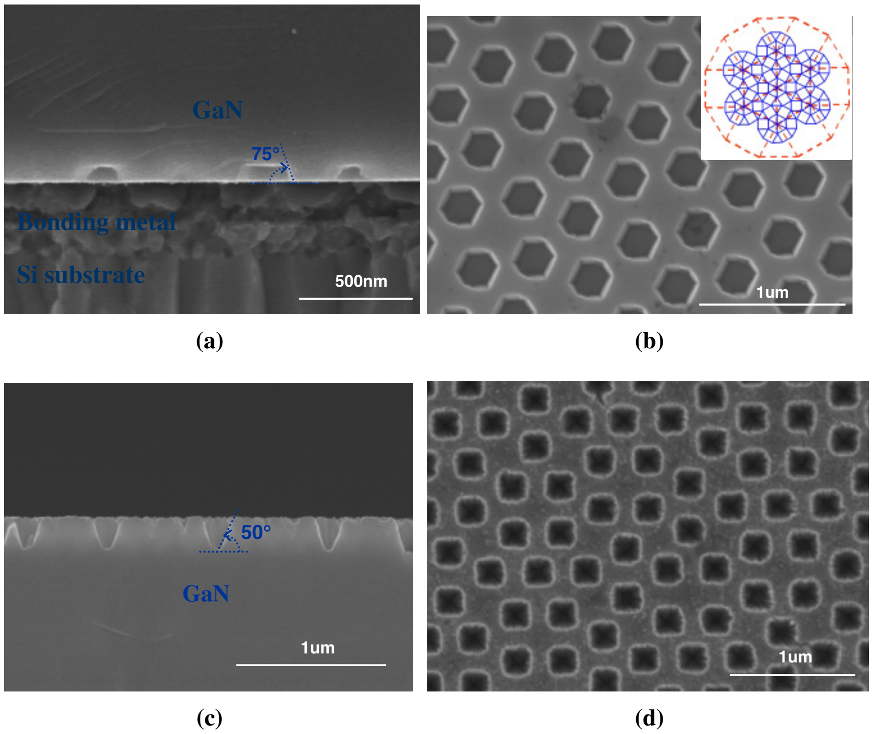

Fig. 2. (Color online) (a) Cross-sectional and (b) top-view SEM images of p-GaN surface with PQC structure [inset shows a schematic diagram of a 12-fold PQC structure on the right-hand-side of (b)]. (c) Cross-sectional and (d) top-view SEM images of n-GaN surface with PQC structure.

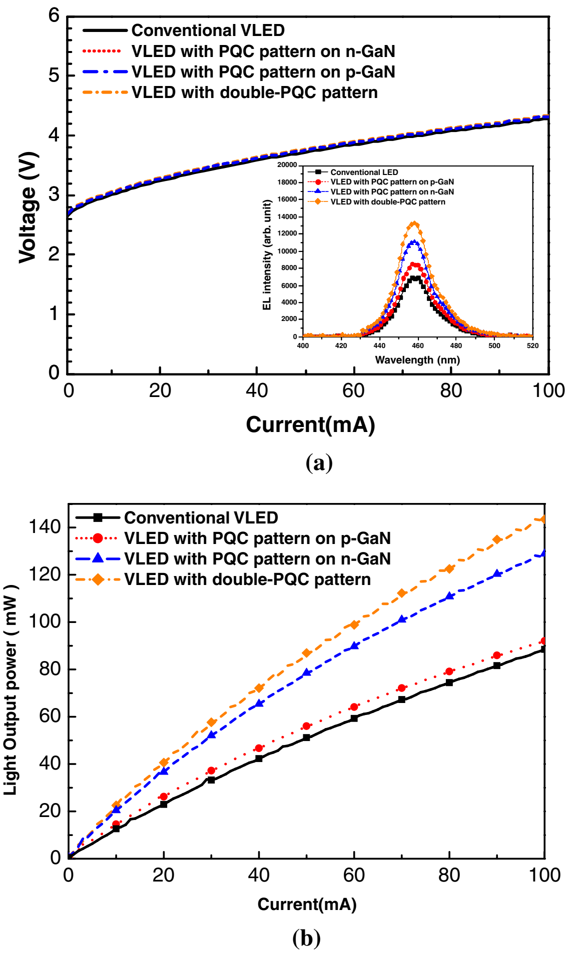

Fig. 3. (Color online) (a) Current–voltage (I–V) (inset shows the room temperature EL spectra at a driving current of 20 mA) and (b) intensity–current (L–I) characteristics of the VLEDs with and without PQC structure.

double-PQC pattern are all higher than that of the conventional VLED. At an injection current of 20 mA, the light output powers of the conventional VLED, the VLED with a PQC pattern on p-GaN, the VLED with a PQC pattern on n-GaN, and the VLED with a double-PQC pattern are 22.9, 26.1, 36.6, and 40.5 mW, respectively. Therefore, the light output powers of the VLED with a PQC pattern on p-GaN, the VLED with a PQC pattern on n-GaN, and the VLED with a double-PQC pattern are enhanced by 14, 60, and 77% compared with that of the conventional VLED. Clearly, this enhancement is attributed to the stronger light scattering effect of the PQC structure on the n-GaN surface and the stronger reflected light effect of the PQC structure on the p-GaN surface. In addition, the corresponding wall plug efficiencies (WPEs) of the conventional VLED, the VLED with a PQC pattern on p-GaN, the VLED with a PQC pattern on n-GaN, and the VLED with a double-PQC pattern are 35, 40, 56, and 61%, respectively, which is a substantial improvement made possible by the use of PQC structures. Note that, for good comparison, the samples we chose are geographically close to each other and the emission peaks of their typical room-temperature EL spectra are all located at 460 nm at a driving current of 20 mA. From Fig. 3(b), guided light can be extracted outside LED chips by scatterings at top transmitted PQC pattern surfaces; therefore, in this case, the extraction probability is larger than that of conventional LEDs. However, the top surface cannot form a perfect PQC pattern using only simple ICP etching, since guided light will propagate inside the LED chip and be partially extracted upon impact on the top transmitted PQC pattern surface. Under such a circumstance, most of the guided light energy will be depleted owing to the absorption of the active region or to mirror loss. When we replace flat Ag reflectors with a PQC pattern on p-GaN surfaces, the

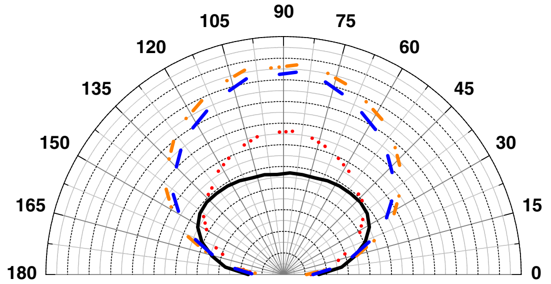

Fig. 4. (Color online) Far-field pattern of the VLEDs with and without PQC structure at a driving current of 20 mA.

situation is different. In Fig. 3(b), guided light emitted towards the PQC pattern and Ag reflectors is scattered. The scattering light will be scattered again by the top transmitted PQC pattern on n-GaN surfaces. Thus, the light emitted from the active region is randomized more effectively, giving more opportunity for photons to escape outside the LED chips. Therefore, a higher guided light scattering efficiency can be achieved by adopting double-PQC pattern surfaces.

To further study the effect of the PQC structure on LED devices, we also measured the light output radiation patterns of the compared VLEDs packaged in TO cans at a driving current of 20 mA, as shown in Fig. 4. It can be seen that the VLED with a PQC pattern on p-GaN, the VLED with a PQC pattern on n-GaN, and the VLED with a double-PQC pattern have much higher extraction efficiencies but a narrower view angle of 130° than the conventional VLED (view angle of 155°). This enhancement is attributed to the strong light beam shaping and reflecting light effect in the vertical direction of the double-PQC structure using NIL. With the higher-fold symmetry (12-fold) of our designed PQC structure, beam shaping through the use of PQC is better than that through the use of a normal photonic crystal structure along azimuth angle.

Figure 4 shows the far-field patterns of the VLED with a PQC pattern on p-GaN, the VLED with a PQC pattern on n-GaN, the VLED with a double-PQC pattern, and conventional LEDs at 20 mA. It is clear from the results that the EL intensities of the VLED with a PQC pattern on n-GaN and the VLED with a double-PQC pattern are larger than those of the VLED with a PQC pattern on p-GaN and conventional LEDs. From Fig. 4, the view angles of the VLED with a PQC pattern on p-GaN, the VLED with a PQC pattern on n-GaN, and the VLED with a double-PQC pattern are almost the same (i.e., 130°); however, the overall integrated areas of the EL intensities of the VLED with a PQC pattern on n-GaN and the VLED with a double-PQC pattern are still larger than that of the VLED with a PQC pattern on p-GaN. However, the view angle of conventional LEDs is larger than those of the VLED with a PQC pattern on p-GaN, the VLED with a PQC pattern on n-GaN, the VLED with a double-PQC pattern, (i.e., 155°); this is due to the non-PQC pattern of the LED in the extraction cone display broad-shaped lobes whose peaks correspond to the Fabry–Perot resonances between the n-GaN reflector and the GaN-air interface. These modes appear as broad resonances in the far-field radiation patterns typical of resonance-cavity LEDs.[17)] From Fig. 4, guided light can be extracted outside LED chips by scatterings at the top transmitted PQC pattern surface; therefore, in this case, the escaping probability of photons is larger than that observed in conventional LEDs. However, the top surface cannot form a perfect PQC pattern using only simple ICP etching, since guided light will propagate inside LED chips and be partially extracted upon impact on the top transmitted PQC pattern surface. Under such a circumstance, most of the guided light energy will be depleted owing to the absorption of the active region or to mirror loss. When we replace flat Ag reflectors with a PQC pattern on p-GaN surfaces, the situation is different. In Fig. 4, guided light emitted towards the PQC pattern and Ag reflectors is scattered. The scattering light is scattered again by the top transmitted PQC pattern on n-GaN surfaces. Thus, the light emitted from the active region is randomized more effectively, giving more opportunity for photons to escape outside the LED chips. Therefore, a higher guided light scattering efficiency is achieved by adopting double-PQC pattern surfaces.[18)]

4. Conclusions

In summary, GaN-based thin-film vertical-injection LEDs with a double-PQC pattern structure incorporating nano-imprint lithography are fabricated. At a driving current of 20 mA and with a chip size of $350 \times 350\,\mu m^2$, the light output power and wall plug efficiency of the VLEDs with a specific double-PQC pattern structure reached 40.5 mW and 61%, which are increased by 77 and 74%, respectively, relative to those of the conventional VLED. The corresponding light radiation pattern shows a narrower beam shape owing to the strong light beam shaping and reflecting light effects of our double 12-fold PQC pattern on the VLED structure.

Acknowledgement

This work is supported by the National Science Council (NSC94-2752-E009-007-PAE, NSC94-2120-M009-007) of the Republic of China.

1) S. Nakamura, M. Senoh, S. Nagahama, N. Iwasa, T. Yamada, T. Matsushita, H. Kiyoku, and Y. Sugimoto: Jpn. J. Appl. Phys. **35** (1996) L74.
2) I. Akasaki, S. Sota, H. H. Sakai, T. Tanaka, M. Koike, and H. Amano: Electron. Lett. **32** (1996) 1105.
3) T. Mukai, M. Yamada, and S. Nakamura: Jpn. J. Appl. Phys. **38** (1999) 3976.
4) C. F. Chu, F. I. Lai, J. T. Chu, C. C. Yu, C. F. Lin, H. C. Kuo, and S. C. Wang: J. Appl. Phys. **95** (2004) 3916.
5) W. Y. Lin, D. S. Wuu, K. F. Pan, S. H. Huang, C. E. Lee, W. K. Wang, S. C. Hsu, Y. Y. Su, S. Y. Huang, and R. H. Horng: IEEE Photonics Technol. Lett. **17** (2005) 1809.
6) C. L. Chang, Y. C. Chung, and C. Y. Liu: Electrochem. Solid-State Lett. **10** (2007) H344.
7) T. Fujii, Y. Gao, R. Sharma, E. L. Hu, S. P. DenBaars, and S. Nakamura: Appl. Phys. Lett. **84** (2004) 855.
8) H. W. Huang, J. T. Chu, C. C. Kao, T. H. Hsueh, C. C. Yu, H. C. Kuo, and S. C. Wang: Nanotechnology **16** (2005) 1844.
9) H. W. Huang, H. C. Kuo, J. T. Chu, C. F. Lai, C. C. Kao, T. C. Lu, S. C. Wang, R. J. Tsai, C. C. Yu, and C. F. Lin: Nanotechnology **17** (2006) 2998.

10) H. W. Huang, C. C. Kao, T. H. Hsueh, C. C. Yu, C. F. Lin, J. T. Chu, H. C. Kuo, and S. C. Wang: Mater. Sci. Eng. B **113** (2004) 125.
11) H. M. Kim, Y. H. Cho, H. S. Lee, S. I. Kim, S. R. Ryu, D. Y. Kim, T. W. Kang, and K. S. Chung: Nano Lett. **4** (2004) 1059.
12) C. F. Lin, J. H. Zheng, Z. J. Yang, J. J. Dai, D. Y. Lin, C. Y. Chang, Z. X. Lai, and C. S. Hong: Appl. Phys. Lett. **88** (2006) 083121.
13) H. S. Chen, D. M. Yeh, Y. C. Lu, C. Y. Chen, C. F. Huang, T. Y. Tang, C. C. Yang, C. S. Wu, and C. D. Chen: Nanotechnology **17** (2006) 1454.
14) M. Tohno, T. Okimoto, Y. Naoi, K. Nishino, S. Sakai, T. Kusuura, A. Mitra, S. Nouda, M. Kimura, S. Kawano, and Y. Muramoto: Proc. 1st Int. Conf. White Light-Emitting Diodes and Solid State Lighting, 2007, p. 370.
15) Z. S. Zhang, B. Zhang, J. Xu, K. Xu, Z. J. Yang, Z. X. Qin, T. J. Yu, and D. P. Yu: Appl. Phys. Lett. **88** (2006) 171103.
16) M. D. B. Charlton, M. E. Zoorob, and T. Lee: Proc. SPIE **6486** (2007) 64860R.
17) J. J. Wierer, A. David, and M. M. Megens: Nat. Photonics **3** (2009) 163.
18) Y. J. Lee, T. C. Lu, H. C. Kuo, and S. C. Wang: J. Disp. Nanotechnol. **3** (2007) 118.